Journal of Thermal Analysis and Calorimetry, Vol. 80 (2005) 225–228

CHARACTERISATION OF THE CATALYTIC PROPERTIES OF CERIA–ZIRCONIA MIXED OXIDES BY TEMPERATURE-PROGRAMMED TECHNIQUES

J. I. Gutiérrez-Ortiz, B. de Rivas, R. López-Fonseca and J. R. González-Velasco[*]

Chemical Technologies for Environmental Sustainability Group, Department of Chemical Engineering,
Faculty of Science and Technology, Universidad del País Vasco/EHU, P.O. Box 644, 48080 Bilbao, Spain

The catalytic properties of ceria–zirconia mixed oxides have been characterised using temperature-programmed techniques such as temperature-programmed desorption of ammonia and water, and temperature-programmed reduction with hydrogen. The acidity and hydrophobicity of these materials increased with zirconia content while the reducibility was maximum for $Ce_{0.5}Zr_{0.5}O_2$ sample.

Keywords: *catalyst, ceria–zirconia mixed oxides, temperature-programmed techniques (TPD, TPR)*

Introduction

Ceria (CeO_2) is a rare earth oxide that has been attracting great interest in the last years due to the redox chemistry of cerium and the high affinity of the element for oxygen that allows wide applications [1]. Particularly, the presence of CeO_2 has been found effective in the promotion of various catalytic reactions including, CO_2 activation, CO oxidation and CO/NO removal. Nowadays, there is much interest in the study of different mixed oxides containing CeO_2, like ceria/zirconia mixed oxides. The use of this type of catalysts as active components of the three-way catalysts for the treatment of exhaust gas from automobiles [2] has recently met a rapid increase. Owing to the number of possible applications of this type of materials, a detailed study of their different types of active sites is of interest.

Experimental

Ceria–zirconia mixed oxides with different molar composition were synthesised by Rhône–Poulenc using a precipitation route from nitrate precursors. The pure ceria sample was also provided by Rhône–Poulenc whereas the pure zirconia sample was supplied from Norton. The pure and mixed oxides were stabilised by calcination in air at 550°C for 4 h, and then pelleted using a hydraulic press ($2.2\cdot10^4$ N cm^{-2}). Finally, pellets were crushed and sieved to obtain grains with 0.3–0.5 mm diameter.

The textural properties were determined by N_2 adsorption–desorption at –196°C in a Micromeritics ASAP 2010 equipment. The samples were previously evacuated overnight at 300°C under high vacuum. A Philips X'PER MPD-System X-ray diffractometer with CuK_α radiation (λ=1.5406 Å) and Ni filter was used for the X-ray diffraction (XRD) studies. Unit cell parameters were estimated from the intensities of lines (111) of CeO_2 and $Ce_xZr_{1-x}O_2$ (x>0.5), (101) of $Ce_xZr_{1-x}O_2$ ($x\leq0.5$) and (111) and (101) of ZrO_2 (monoclinic and tetragonal structure, respectively).

A Micromeritics AutoChem 2910 instrument was used for temperature-programmed investigations. Prior to analysis the samples were first calcinated at 550°C in a 5% O_2/He stream and then cooled down in a N_2 flow. The temperature-programmed desorption (TPD) analysis required a previous saturation of the sample with the respective probe molecule followed by removal of physisorbed species with a desorption treatment in a He stream at 10 K min^{-1} heating rate from 100 to 550°C.

The 10 K min^{-1} temperature-programmed reduction (TPR) was carried out under an Ar+5% H_2 flow from 50 to 950°C.

Results and discussion

Table 1 summarises the textural properties of the investigated ceria–zirconia mixed oxide catalysts. Table 1 data show a surface area of about 100 m^2 g^{-1} in the composition range 50–80% CeO_2, whereas 86 and 51 m^2 g^{-1} are the values found for 15% CeO_2 and pure ZrO_2, respectively. Composition and pore size seem not clearly correlated to each other, possibly because of the transition from cubic to tetragonal

---

[*] Author for correspondence: iqpgovej@lg.ehu.es

1388–6150/$20.00

Akadémiai Kiadó, Budapest, Hungary
Springer, Dordrecht, The Netherlands

Table 1 Main physico-chemical properties of $Ce_xZr_{1-x}O_2$ mixed oxides

	BET surface area/$m^2\ g^{-1}$	Pore volume/$cm^3\ g^{-1}$	Average pore size/Å	Lattice parameter/Å
CeO_2	99	0.21	59	5.41
$Ce_{0.8}Zr_{0.2}O_2$	102	0.18	48	5.35
$Ce_{0.68}Zr_{0.32}O_2$	101	0.24	70	5.30
$Ce_{0.50}Zr_{0.50}O_2$	99	0.21	64	5.26
$Ce_{0.15}Zr_{0.85}O_2$	86	0.28	102	5.14
ZrO_2	51	0.25	157	–

structure on increasing ZrO_2 content [3] with substantial changes in the pore size.

The X-ray diffraction patterns are shown in Fig. 1. The CeO_2 sample showed well-defined peaks corresponding to a cubic structure. However, it should be pointed out that the most intense lines were shifted to significantly higher diffraction angles with increasing ZrO_2 content, a finding that may be related to the shrinkage of the lattice on replacing Ce^{4+} with smaller Zr^{4+} ions [4]. The mixed oxide systems is a solid solution where the cation sublattice was found to form cubic and tetragonal structure for $x \geq 0.68$ and $x \leq 0.5$, respectively, whereas pure ZrO_2 is monoclinic. The cell parameter for the $Ce_xZr_{1-x}O_2$ mixed oxides calculated from the main diffraction peaks are listed in Table 1. A linear decrease of a_0 was observed with increasing ZrO_2 content, in agreement with the Vegard rule, the Zr^{4+} ionic radius (0.084 nm) being smaller than that of Ce^{4+} (0.098 nm) [5].

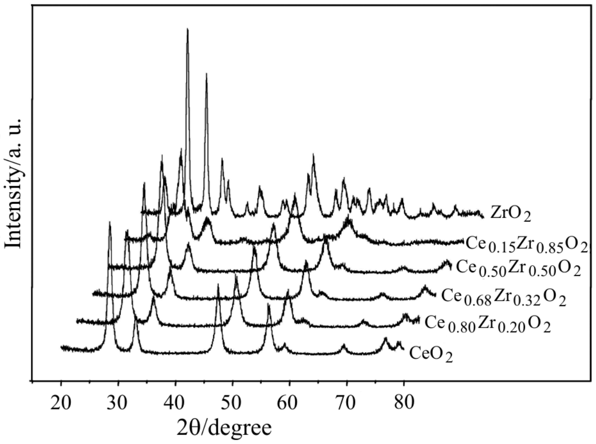

Fig. 1 X-ray diffraction patterns of $Ce_xZr_{1-x}O_2$ mixed oxides

Acid sites play an important role in the adsorption and reaction of different type of hydrocarbons on the surfaces of ceria and CeO_2-containing materials. TPD of ammonia allowed evaluation of the acidic properties of the different samples. It is well-known that chemical mixing with another oxide can significantly change the acid-base properties of a given metal oxide [6, 7]. Addition of zirconium into the ceria lattice was therefore supposed to have a complex influence on the acidity of the pure parent oxide. The total concentration of acid sites was calculated as the amount of ammonia adsorbed per gramm (Table 2). The total acidity, which was the lowest for pure ceria, markedly increased on adding ZrO_2. The highest acidity was accordingly found for the mixed oxide with the highest ZrO_2 content ($Ce_{0.15}Zr_{0.85}O_2$). The NH_3-TPD profiles shown in Fig. 2 revealed the presence of acid sites with varying strength on each sample. An attempt to characterise the strength of acid sites was carried out by means of a deconvolution of the TPD profiles into four gaussian peaks. The desorption peaks were located at around 160, 240, 385, 535°C, respectively, irrespective of the catalyst. The peaks at 160 and 240°C were related to the weak acidity present in the catalysts while the other two peaks were assigned to strong acidity. The sum of the areas under the first two peaks was assumed to be the number of weak acid sites and the sum of the areas under the other peaks was associated with the number of strong acid sites. It was noticed that the contribution

Table 2 Results for temperature-programmed analysis of $Ce_xZr_{1-x}O_2$ solid solutions

	Consumption of H_2/ μmol g^{-1}	Total acidity/ mmol $NH_3\ g^{-1}$	Strong sites/ mmol $NH_3\ g^{-1}$	Weak sites/ mmol $NH_3\ g^{-1}$	H_2O adsorption/ mmol g^{-1}
CeO_2	196	0.17	0.03	0.14	1.45
$Ce_{0.8}Zr_{0.2}O_2$	1004	0.24	0.09	0.15	2.04
$Ce_{0.68}Zr_{0.32}O_2$	1293	0.26	0.10	0.16	2.10
$Ce_{0.50}Zr_{0.50}O_2$	1322	0.31	0.13	0.18	2.22
$Ce_{0.15}Zr_{0.85}O_2$	509	0.35	0.15	0.20	2.64
ZrO_2	–	0.24	0.11	0.13	2.06

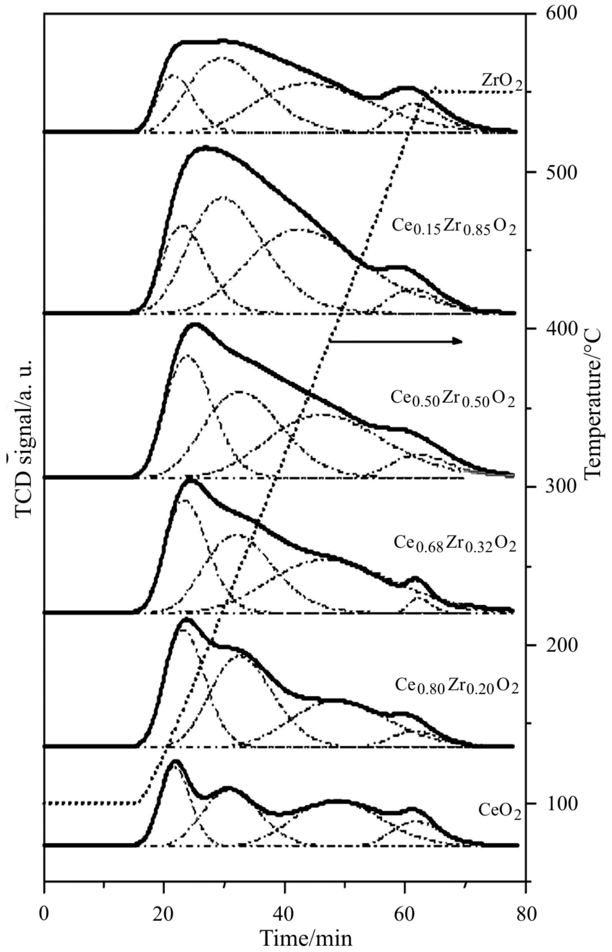

Fig. 2 NH_3-TPD profiles of $Ce_xZr_{1-x}O_2$ mixed oxides

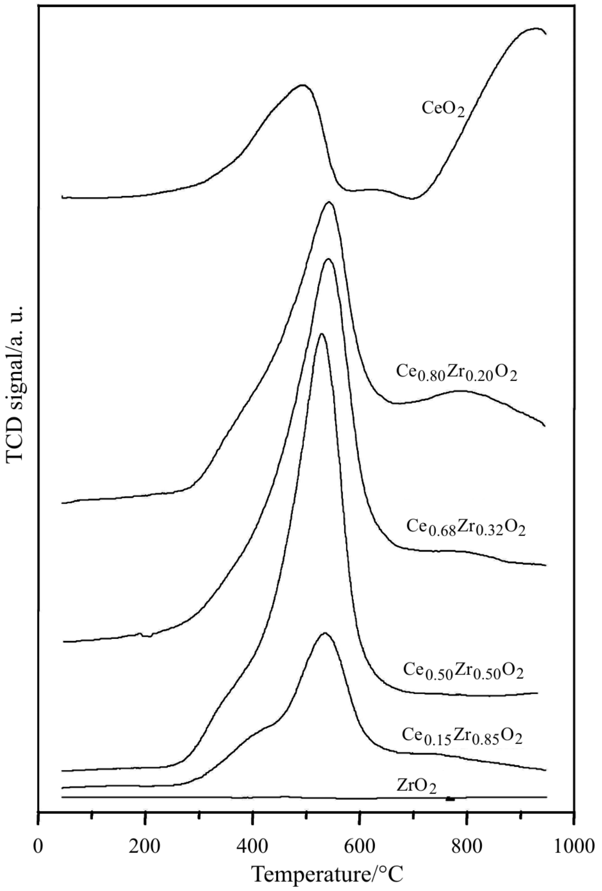

Fig. 3 H_2-TPR profiles of $Ce_xZr_{1-x}O_2$ mixed oxides

to the total acidity was larger at larger ZrO_2 contents. Accordingly, the $Ce_{0.15}Zr_{0.85}O_2$ sample presented the highest amount of strong acid sites (Table 2).

TPR with hydrogen has been widely employed in order to characterise the reducibility of ceria-based materials. Cerium oxide is well-known for its easier reducibility if compared to other fluorite-type oxides [8]. The hydrogen consumption was quantified by integrating the area beneath the whole profile (Table 2). The TPR profile of ceria showed a two-peak pattern, suggesting that reduction of ceria may follow a two-step process. The first low temperature signal at ca. 500°C was assigned to the reduction of the surface, while reduction of the bulk was proposed as the cause of the high-temperature signal at ca. 900°C. The TPR profiles of the mixed oxides essentially showed a main broad reduction signal in agreement with the expectation of an enhanced reduction of the bulk mixed oxide when doped with ZrO_2. Indeed, the insertion of ZrO_2 into the cubic CeO_2 resulted in a distortion on the mixed oxide structure, as revealed by XRD analysis. As a consequence, the reduction was no longer confined to the surface but involved the deep bulk too. Figure 3 clearly shows the change of the reduction behaviour of CeO_2 as the main hydrogen consumption was shifted to lower temperatures [9, 10]. It is worth pointing out that there was no contribution from the reduction of ZrO_2.

The reduction process of a cerium atom in a ceria–zirconia mixed oxide occurred according to the following equation:

$$Ce_xZr_{1-x}O_2+\delta H_2 \leftrightarrow Ce_xZr_{1-x}O_{2-\delta}+\delta H_2O+\delta V_o \quad (1)$$

where the elimination of the capping oxygen anion as water molecules involved the appearance of an oxygen vacancy (V_o). The presence of those vacancies considerably promoted the mobility of oxygen from the bulk to the surface. Therefore, a measurement of the hydrogen consumption was proportional to the amount of Ce^{3+} formed, and also proportional to the amount of oxygen vacancies, which was related to the oxygen mobility [11, 12]. Since the reduction occurred to the largest extent for $Ce_{0.5}Zr_{0.5}O_2$, the oxygen mobility was more noticeably promoted for this catalyst.

Many catalytic processes involve formation of water vapour, which therefore is worth determining. For this reason, in some cases hydrophobic materials

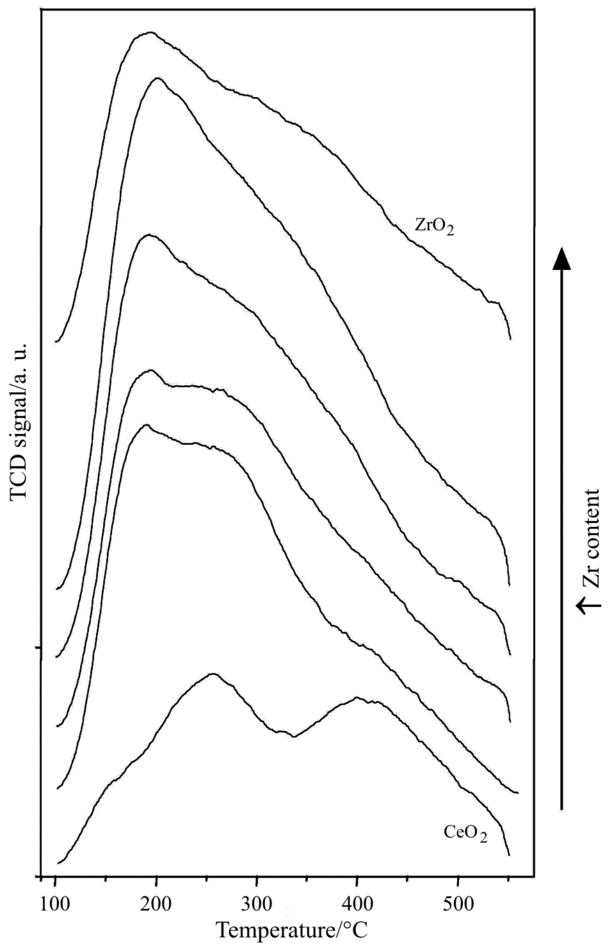

Fig. 4 H$_2$O-TPD profiles of Ce$_x$Zr$_{1-x}$O$_2$ mixed oxides

are beneficial in processes where high water vapour concentrations are present, either by offering reduced sensitivity to water inhibition of active sites, or by enhanced hydrothermal stability where other materials like silica or alumina would be unsuitable [13–15]. In this work, temperature programmed desorption (TPD) of water was carried out to evaluate the hydrophobic or hydrophilic character of ceria–zirconia mixed oxides.

Figure 4 shows the H$_2$O-TPD profiles in the range 100–550°C, whereas the amount of water adsorbed per gramm is reported in Table 2. These findings suggest that pure ceria is the catalyst which adsorbed the lowest amount of water and the hydrophilicity of the mixed oxide increased with zirconia content.

Conclusions

The characterisation of the catalytic sites of ceria–zirconia solid solutions with varying Ce/Zr by means of temperature-programmed techniques led to the following conclusions. The total acidity and the ratio between strong/total acidity was larger as the zirconia content was increased. Similarly, the water adsorption capacity was enhanced with zirconia content. On the other hand, the oxygen mobility of the mixed oxide was the highest for Ce$_{0.5}$Zr$_{0.5}$O$_2$ sample.

Acknowledgements

The authors wish to thank Universidad del País Vasco/EHU (9/UPV13517/2001) and Ministerio de Ciencia y Tecnología (PPQ2001-0543) for the financial support.

References

1 L. F. B. Malta, V. R. Caffarena, M. E. Medeiros and T. Ogasawara, J. Therm. Anal. Cal., 75 (2004) 901.
2 J. R. González-Velasco, M. A. Gutiérrez-Ortiz, J. L. Marc, J. A. Botas, M. P. González-Marcos and G. Blanchard, Top. Catal., 16–17 (2001) 101.
3 J. R. González-Velasco, M. A. Gutiérrez-Ortiz, J. L. Marc, J. A. Botas, M. P. González-Marcos and G. Blanchard, Appl. Catal. B, 22 (1999) 167.
4 A. E. Nelson and K. H. Schulz, Appl. Surf. Sci., 210 (2003) 206.
5 B. M. Reddy, A. Khan, Y. Yamada, T. Kobayashi, S. Loridant and J.-C. Volta, J. Phys. Chem. B, 107 (2003) 11475.
6 M. G. Cutrufello, I. Ferino, R. Monaci, E. Rombi and V. Solinas, Top. Catal., 19 (2002) 225.
7 J.-Y. Miao, L.-F. Yang and J.-X. Cai, Surf. Interface Anal., 28 (1999) 123.
8 A. Tschöpe, W. Liu, M. Flytzani-Stephanopoulos and J. Y. Ying, J. Catal., 157 (1995) 42.
9 M. Boaro, M. Vicario, C. de Leitenburg, G. Dolcetti and A. Trovarelli, Catal. Today, 77 (2003) 407.
10 Y. Madier, C. Descorme, A. M. Le Govic and D. Duprez, J. Phys. Chem. B, 103 (1999) 10999.
11 G. Balducci, J. Kaspar, P. Fornasiero and M. Graziani, J. Phys. Chem. B, 101 (1997) 1750.
12 N. Sergent, P. Gélin, L. Périer-Camby, H. Praliaud and G. Thomas, J. Therm. Anal. Cal., 72 (2003) 1117.
13 P.-O. Larsson and A. Andersson, J. Catal., 179 (1998) 72.
14 M. T. Vandersall, S. G. Maroldo, W. H. Brendley, K. Jurczyk Jr. and R. S. Drago, ACS Symp. Ser., 552 (1994) 331.
15 G. W. Chadzynski, D. Sternik, P. Staszczuk and B. Kucharczyk, J. Therm. Anal. Cal., 78 (2004) 441.